Symmetry breaking and electrostatic attraction between two identical surfaces

F. Plouraboué
Université de Toulouse, INPT, UPS, IMFT (Institut de Mécanique des Fluides de Toulouse), Allés Camille Soula, F-31400 Toulouse, France
and CNRS, IMFT, F-31400 Toulouse, France

H.-C. Chang
Center for Microfluidics and Medical Diagnostics and Department of Chemical and Biomolecular Engineering, University of Notre Dame, Notre Dame, Indiana 46556, USA
(Received 14 November 2008; published 16 April 2009)

By allowing the surface charge of one surface to affect the adsorption equilibrium of the other, we establish the existence of a long-range attractive interaction between two identical surfaces in an electrolyte containing polyvalent counterions with a mean-field Poisson-Boltzmann approach. A Stern electrostatic condition from linearization of the mass-action adsorption isotherm is used to capture how polyvalent ion condensation affects and reverses the surface charge. We furthermore establish a direct mapping between this Stern-layer condition and previously derived modified mean-field formulations associated with correlated fluctuations theory. For a sufficiently potential-sensitive isotherm, antisymmetric charge inversion can occur to produce an attractive force that increases with decreasing ionic strengths. Analyses of a mass-action isotherm produce force-separation relations, including an exponential far-field force decay distinct but consistent with previously proposed correlated fluctuation theories and in quantitative agreement with experimental data.

I. INTRODUCTION

Recent atomic force microscopy (AFM) studies have shown that, in the presence of a polyvalent counterion, two similarly charged or identical surfaces can develop an attractive force at a distance comparable to the Debye screening length λ [1,2]. This observation is most likely related to earlier reports on attraction between identical colloids in an electrolyte, although the role of polyvalency is not as well established for colloids [3,4]. It is also related to the condensation of like-charged molecules such as DNAs [5]. It has been rigorously shown that, for two identical spheres with constant potential [6] or constant surface field [7], the interparticle interaction is necessarily repulsive according to the classical Poisson-Boltzmann (PB) mean-field theory [6]. For this reason, theories for like-charge attraction phenomena have sought mechanisms beyond the classical mean-field description to include spatial correlation of charge fluctuations [8–11].

Such fluctuation theories suggest cross-surface spatial correlation either between fluctuations of the condensed counterions in the Stern layer [12] or between surface Wigner crystals [13] that are formed by the same ions. However, when the two surfaces are separated by a distance larger than the Bjerrum length, thermal noise is expected to disrupt the fluctuation correlation of condensed ions on the two surfaces. Also strong concentration gradients develop within the Debye layer which may invalidate the assumptions of many correlated fluctuation theories.

Instead, one expects mean-field theory to be valid at separations comparable to the Debye length, when it is much larger than the Bjerrum length. Spatial correlation of fluctuations between the condensed charge and the surface charge on the same surface, which is over a distance comparable to or shorter than the Bjerrum length, affects the local screening and charge inversion [14]. This is particularly true for polyvalent counterions, which can cause local charge inversion and whose fluctuations are known to be important. Indeed, the two-fluid model for free/condensed counterions proposed in [10] shows, with a modified mean-field theory, that the surface potential and the charge might be coupled by fluctuations on the condensed plates. Nevertheless this coupling was not previously considered in [10] where a zero potential is prescribed at the boundaries. Hence, long-range attraction over large Debye layers is quite distinct from bridging of both surfaces by the polyvalent counterion over short Stern-layer separations [15].

Although AFM measurements of [1] and recent molecular-dynamics (MD) simulation of DNA condensation does not show surface ion ordering [16], correlated fluctuations should nevertheless play a role during ion condensation onto charged surfaces [17] especially for polyvalent electrolytes counterions [2].

However, connecting the fluctuations at a Bjerrum length separation from the surface to longer-range attraction over the Debye length is still unclear. More specifically, theories for correlated layers charges between two parallel plates separated by a distance $2h$ much larger than the Debye length λ give rises to an effective "long-range" dipolar attractive pressure, $p \sim 1/(2h)^3$ [18], an almost dipolar one $p \sim \ln[2h/\lambda]/(2h)^3$ [8,10], or a modified exponential attraction $p \sim \exp(-4h/\lambda)/2h$ [19,20], also found in colloids interactions [21]–whereas the classical Derjaguin-Landau-Verwey-Overbeek (DLVO) theory only predicts a repulsive exponential behavior $p \sim \exp(-2h/\lambda)$.

In this paper, we lump short-range correlated fluctuation effects into a linear empirical isotherm for polyvalent counterion condensation that captures charge inversion. We then show that this linear Stern isotherm condition can induce asymmetric charge inversion and PB ion distributions due to

nonlinear field screening/enhancement of the space charge and field-enhanced condensation effects on the two surfaces.

Moreover, we are able to show that, despite the simplicity of the model, the resulting force-separation relations display a variety of attractive/repulsive patterns which are quantitatively consistent with AFM measurements in the same polyvalent electrolyte. Fundamental to the theory is the observation that, for separation less than or comparable to λ, the field from one surface can affect the adsorption equilibrium and the Stern-layer potential on the other. The field transmission across the large Debye layer separation with large concentration gradients must be described by a mean-field theory. For nearly neutral surfaces near the isoelectric point, where charge inversion is possible, it is shown that these two surfaces necessarily undergo opposite charge reversal to produce an attractive interaction. This attraction can be overwhelmed if the native charge density is too high to allow charge reversal on one of the surfaces. The paper is organized as follows. We describe in Sec. II A the classical Stern-layer boundary condition in its usual formulation. We then establish in Sec. II B a one-to-one mapping between Stern-layer parameters and a statistical mechanics two-fluid model previously proposed for fluctuation theory. In Sec. III we first discuss the linear Debye-Hückel (D-H) approximation with Stern layers in order to find the bifurcation points for the nonlinear Poisson-Boltzmann solutions which are further analyzed analytically in Sec. III B. Sec. IV is devoted to the numerical computation of the main characteristics of these solutions such as the surface potential and the interaction force with Stern-layer parameters and dimensionless gap. Finally our findings are compared with available experimental data in Sec. VI. We first show in Sec. VI A that adsorption isotherm linearization leads to Stern-layer parameter consistent with those obtained in Sec. II B. We then compare long-range and intermediate range force behavior predicted by our theory with experimental measurements in Sec. VI B.

II. MODIFIED MEAN-FIELD DESCRIPTION

In this section we first described the classical Stern-layer condition to account for ion condensation at the solid surface and its relation to adsorption isotherms. We then present in detail the statistical mechanical two-fluid model of Lau and Pincus [10] for counterion condensation. We then establish its equivalence, at the mean-field level, with a Stern-layer boundary condition, when considering Neumann boundary condition rather than the previously considered homogeneous Dirichlet.

A. Stern-layer boundary condition

Assuming rapid polyvalent counterion condensation kinetics, the isotherm stipulates that the surface charge density σ on a surface is a function of the Stern-layer potential ϕ and the bulk electrolyte concentrations. The potential ϕ represents the electrical potential difference between a bulk charge with a zero reference potential and that of a condensed/adsorbed polyvalent counterion on the surface in the presence of an electric field. The condensed state then represents a free energy minimum, where the free energy includes the above electric potential, the entropy loss due to condensation, and the interaction potential among the counterions and the surface. All three quantities are complex functions of the condensed polyvalent counterion condensation. As such, the free energy minimum represents a complex isotherm relationship for the equilibrium condensed counterion concentration as a nonlinear function of the potential difference and the bulk concentration. The surface charge σ is then the sum of the original field-free surface charge and those of the condensed counterions. A typical calculation of the nonlinear isotherm for the net charge density has been done by Zohar *et al.* [1] and is shown in Sec. VI. It contains various equilibrium association and dissociation constants for the counterion condensation reaction—the mutual interaction of the condensed counterions and the surface-counterion interaction. The net surface charge σ vanishes at a particular isoelectric potential ϕ_0 where the field-induced condensation has reversed the surface charge.

At a given bulk electrolyte concentration, σ is a nonlinear function of ϕ. One can, however, linearize this expression at the isoelectric potential ϕ_0 to obtain a σ that is proportional to $\phi-\phi_0$. Using a Gauss volume that confines the condensed charges within the Stern layer and assuming there is no field on the solid side, a simple integration of the Poisson equation indicates that this net charge σ is proportional to the normal surface electric field just outside the condensed ions $\partial_z\phi$. If we now assign this normal field outside the condensed Stern layer as the boundary condition for the Poisson equation beyond it, we obtain

$$\partial_z\phi = \pm K[\phi - \phi_0], \tag{1}$$

where the inverse Stern slip length K is determined by various association/dissociation equilibrium constants of participating ions and the isoelectric potential ϕ_0 represents the compensate Zeta potential on the true surface due to polyvalent ion condensation.

The Stern slip length can take on either sign, depending on the charge of the polyvalent counterion, the monovalent counterions, the uncompensated surface, and the complex interaction (chemistry) among them. In Stern's classical context, this boundary condition represents the field across the Stern layer with the condensed counterion and ϕ_0 is the potential just outside the Stern layer. The inverse Stern slip length K is then related to the thickness of the condensed layer and the surface density of the condensed counterions, with different signs accounting for the charge of the polyvalent counterion. Our analysis is for two planar surfaces, although extension to spheres can be carried out with the classical Derjaguin formulation. We scale the normal coordinate z by h the half-separation between the two surfaces and the potentials ϕ and ϕ_0 by $RT/ZF=k_BT/Ze$, the thermal energy per valency measured in electric potential, where R is the ideal gas constant, T is the temperature, Z is the monovalent counterions valency, F is the Faraday constant, k_B is the Boltzmann constant, and e is the electron charge. From this we obtain an expression identical to Eq. (1) but with dimensionless variables,

$$\partial_z\phi(\pm 1) = \pm\mu\sqrt{\beta}[\phi(\pm 1) - \phi_0], \tag{2}$$

where we define the dimensionless separation squared as $\beta = (h/\lambda)^2$ so that the dimensionless K in Eq. (1), scaled by the separation h has been decomposed in $K = -\mu\sqrt{\beta}$ such that μ is only a function of the electrolyte composition. The magnitude of μ measures the effect of the Stern-layer potential (and external field) on the adsorption isotherm.

With the same scaling, the PB equation for symmetric electrolytes is

$$\partial_z^2\phi = \beta \sinh \phi, \tag{3}$$

which will be solved with Eq. (2) for $z = \pm 1$. We note that Eqs. (2) and (3) are symmetric to the transformation $\mu \to -\mu$ and $z \to -z$. Hence the sign of μ is arbitrary and will be taken to be negative so that μ is a positive constant. For any value of ϕ_0, symmetric solutions always exit, but antisymmetric solutions are only permitted for $\phi_0 = 0$.

B. Equivalence with "two-fluid" counterions condensation models

Let us first give here a brief description of the two-fluid model analyzed in [10,11,22]. The counterions of a charged solution are divided into a condensed fraction of charges of surface density n_c and a prescribed surface charge density n_0. The condensed charges are trapped onto the surface while the free charges can move into the bulk fluid. The surface density of the condensed counterions n_c is not *a priori* prescribed but results from the balance between electrostatic interactions and fluctuations. In the frame of a pointlike particles description on the surface the condensed counterions n_c has been computed in [10,22] from the functional minimization of the free energy which includes two-dimensional (2D) and three-dimensional (3D) entropic and electrostatic contributions. It has been found in [22] that correlation effects are responsible for a first-order phase transition of the condensed phase, when varying the surface charge order parameter $g = \pi Z^3 \ell_B^2 n_0$, where Z is the ion valency, ℓ_B is the Bjerrum length defined by $\ell_B \equiv e^2/\epsilon k_B T$ associated with the electron charge e, permittivity ϵ, Boltzmann constant k_B and the temperature T. From the cubic dependence of g on Z, it is clear that the condensation is very sensitive to the ion valency, as quantitatively observed in many experiments. The minimization of the free energy of the 2D and 3D entropic and electrostatic contributions leads to a modified mean-field equation for the mean-field potential ϕ. This modified mean-field equation has been written for single counterion in Eq. (17) of [10] and straightforwardly extended to electrolyte solution in [11]. We write their modified mean-field equation in dimensionless parameters for condensed counterions in a electrolyte placed between two plates located at position $z = \pm 1$,

$$\partial_z^2\phi - \beta \sinh \phi = \frac{n_R \ell_B h}{Z} \sum_{\pm} \delta(z = \pm 1) + \pi Z^2 n_c \ell_B h \sum_{\pm} \delta(z = \pm 1)\phi(z), \tag{4}$$

where δ stands for the Dirac distribution. The two terms of the right-hand side of Eq. (4) have two distinct origins. The first one is associated with the pointlike contribution of the condensed charges onto the surfaces which naturally result from an electrostatic contribution. It is nevertheless interesting to note that the prefactor of this term is not the obvious imposed surface charge density n_0 but the bare charge n_R which results from the renormalized bare surface charge density $n_R = (n_0 - Z n_c)$. The second term results from the fluctuation contribution to the condensate and couples the mean-field potential to the condensate surface charge. The contribution of this second term to the surface interaction has been previously ignored in [10,11,22] from imposing a zero potential boundary condition $\phi(\pm 1) = 0$ for the PB mean-field ϕ. Hence, by using a Dirichlet boundary condition which annihilates the contribution of the second term of Eq. (4) right-hand side, previous studies have then prescribed a zero contribution of the fluctuation dependence of the mean-field solutions. They subsequently analyzed the challenging estimate of fluctuations contribution to the attraction between surfaces, while discarding their influence at the mean-field level.

Our contribution in this paper is to show that keeping with the modified mean-field description is enough to satisfactorily describe most of the experimental observations on chargedlike attraction. We now first show how modified mean-field description (4) is formally equivalent with Stern-layer boundary condition (2). Instead of considering strong formulation (4), let us now establish the weak formulation of this nonlinear elliptic problem associated with the dual test functions Φ. Using notation $\langle \phi, \Phi \rangle \equiv \int_{-1}^{1} \phi \Phi dz$ and integrating the weak formulation of Eq. (4) by parts one gets

$$-\langle \partial_z\phi, \partial_z\Phi \rangle - \beta \langle \sinh \phi, \Phi \rangle = \left[\mathrm{sgn}(-z)\partial_z\phi + \frac{n_R \ell_B h}{Z} + \pi Z^2 \ell_B n_c h \phi, \Phi \right], \tag{5}$$

where we have used notation $[u, \Phi] \equiv u(-1)\Phi(-1) + u(1)\Phi(1)$, and $\mathrm{sgn}(z)$ stands for the sign of variable z. It can be seen in this weak formulation that the source terms of Eq. (4) are associated with the second constant term and third linear variation with $\phi(\pm 1)$ on the right-hand side of Eq. (5). Now, using the same weak formulation for PB Eq. (3) but prescribing Stern-layer boundary condition (2) leads to the following problem:

$$-\langle \partial_z\phi, \partial_z\Phi \rangle - \beta \langle \sinh \phi, \Phi \rangle = [\mathrm{sgn}(-z)\partial_z\phi, \Phi] = [\mu\sqrt{\beta}\phi_0 + \mu\sqrt{\beta}\phi, \Phi], \tag{6}$$

where again we have used notation $[u, \Phi] \equiv u(-1)\Phi(-1) + u(1)\Phi(1)$ on the right-hand side of Eq. (6). From the inspection of weak formulations (5) and (6) one can see that there is a possibility for these two problems to be formally equivalent. If one uses Neumann boundary conditions $\partial_z\phi(\pm 1) = 0$ in problem (4), then the first term on the right-hand side of Eq. (5) cancels out. In this case, formulations (5) and (6) can be exactly mapped one onto another provided that the parameters μ and ϕ_0 fulfill

$$\mu = \pi Z^2 \ell_B \lambda n_c, \tag{7}$$

$$\phi_0 = \frac{n_R}{n_c \pi Z^3}. \tag{8}$$

Relations (7) and (8) then provide a statistical mechanics based Stern-layer formulation that we have not been able to find elsewhere in the previous literature. Parameters μ and ϕ_0 then depend on the Bjerrum length ℓ_B, the ions valency Z, the condensed surface charge n_c, and the effective bare surface charge n_R. n_c and n_R also depends on the order parameter $g=\pi Z^3 \ell_B^2 n_0$ through a first-order transition and have been computed numerically and asymptotically in certain limits in [22]. Finally it is interesting to note that prescribing a Neumann boundary condition to the weak formulations [Eq. (5)] is not necessary to obtain the equivalence between Stern-layer formulations (2) and (3) and two-phase model (4). A mathematical alternative for this equivalence could have been to apply another Stern-layer boundary condition for the potential $\partial_z \phi(\pm 1) = \pm[a + b\phi(\pm 1)]$ in weak formulation (5) associated with problem (4). Nevertheless such alternative introduces two supplementary unknown coefficients and does not seen physically relevant. In Sec. VI A we will prefer to derive these parameters from the adsorption isotherm linearization parameters, which are more easy to relate to some given experimental condition.

III. SOLUTION TO THE PB PROBLEM WITH STERN LAYERS

In this section we solve the PB problem associated with boundary condition (2). We first investigate the linear approximation associated with the D-H approximation and then explore the features of the solution to the full nonlinear problem.

A. D-H approximation

Even though the linearized version of Eq. (3) does not produce any interaction, we still use the linear D-H approximation to determine the bifurcation of nontrivial solutions. Two linearized solutions exist, one symmetric (denoted with a capital S) and one nonsymmetric (denoted with NS) with respect to reflection across midplane,

$$\phi^S = \cosh(\sqrt{\beta} z), \tag{9}$$

$$\phi^{NS} = \frac{e^{\sqrt{\beta} z}}{2} + \left(\frac{2\mu\phi_0}{\sqrt{\mu^2 - 1}} - 1 \right) \frac{e^{-\sqrt{\beta} z}}{2}. \tag{10}$$

The coefficients of these eigenfunctions cannot be specified for the homogenized versions of Eqs. (2) and (3). However, the corresponding linear operator becomes singular at

$$\beta_c^S = \left(\ln \left[\frac{-\mu\phi_0 + \sqrt{\mu^2\phi_0^2 + (1-\mu^2)}}{(1-\mu)} \right] \right)^2, \tag{11}$$

$$\beta_c^{\mathrm{NS}} = \left(\frac{1}{2} \ln \frac{\mu+1}{\mu-1} \right)^2, \tag{12}$$

where nontrivial solutions can bifurcate from the trivial solution 0. We note that for nonsymmetric solutions (antisymmetric in the case $\phi_0 = 0$), only $|\mu| > 1$ is possible, or, more precisely, $\mu > 1$ since we are restricted to positive μ values.

B. Solution to Poisson-Boltzmann problem

Equation (3) is integrable and its first integral is

$$\frac{1}{2}(\partial_z \phi)^2 = \beta \cosh \phi + d, \tag{13}$$

where d is a constant which depends on μ, β, ϕ_0 and the surface potential. Evaluating this integral at $z = \pm 1$ as a reference point, one obtains

$$d' = \frac{d}{\beta} = \frac{1}{2}\{\mu[\phi(\pm 1) - \phi_0]\}^2 - \cosh \phi(\pm 1). \tag{14}$$

This parameter can be related to the force between the two surfaces. Using Green's theorem and including the osmotic pressure from the bulk solution at the infinities behind the two surfaces [6], the pressure (force per unit area) between the two surfaces can be derived;

$$p = \left[-\tfrac{1}{2\beta}(\partial_z \phi)^2 + \cosh \phi - 1 \right] = -d' - 1,$$

$$p = -\tfrac{[\mu(\phi(1) - \phi_0)]^2}{2} + \cosh \phi(1) - 1, \tag{15}$$

where the dimensionless pressure p has been normalized by the Debye Maxwell stress $\epsilon(RT/zF\lambda)^2$ for convenience to remove the dependence on separation. It is independent of z and hence its value at $z=1$ is evaluated by using Eq. (14). Looking at the last expression of Eq. (15) it is obvious that the osmotic pressure difference in the second term is always repulsive and the Maxwell pressure in the first term is always attractive, leading apparently to possible attractive or repulsive forces depending on $\phi(1)$ or d'. Nevertheless it can be easily shown by evaluating the pressure at $z=0$ for the case of $\phi(0)=0$ associated with antisymmetric solution for $\phi_0 = 0$ in the first expression of Eq. (15) that the only remaining term at the origin is the attractive Maxwell pressure. Hence all antisymmetric solutions near the isoelectric point are attractive. Furthermore, some observations can be made at the (D-H) limit of small $\phi(1)$. Expansion of the osmotic pressure term shows that attractive interaction is only possible for $\mu > 1$, which is consistent with the previous observation that antisymmetric solutions are only possible for this parameter range.

The required solution can be simplified by the Boltzmann transformation

$$\psi = \exp(-\phi/2), \tag{16}$$

such that first integral (13) is transformed into

$$\partial_z \psi = \pm \tfrac{\sqrt{\beta}}{2} \sqrt{\psi^4 + 2\tfrac{d}{\beta}\psi^2 + 1},$$

$$\partial_z \psi = \pm \tfrac{\sqrt{\beta}}{2} \sqrt{(\psi^2 - \alpha_-)(\psi^2 - \alpha_+)}, \tag{17}$$

where,

$$\alpha_\pm = -d' \pm \sqrt{d'^2 - 1}, \tag{18}$$

are complex conjugate roots. Integrating Eq. (17) one more time leads to

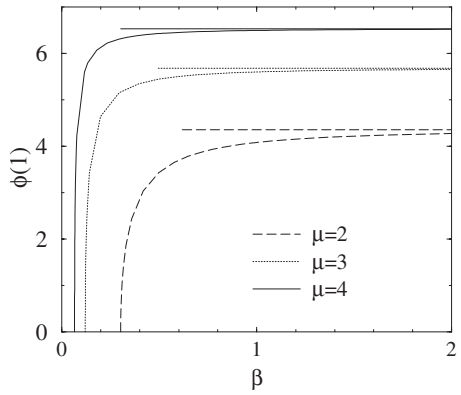

FIG. 1. Surface potential of asymmetric solution $\phi(1)$ at $z=1$ versus dimensionless gap β for $\phi_0=0$. The dotted lines display the value $\phi^{\infty}(1)$ obtained from solving (21).

$$\pm\frac{\sqrt{\beta}z}{2}+c=-\sqrt{\alpha_-}F_1(\psi\sqrt{\alpha_+},\alpha_-), \tag{19}$$

where F_1 is the elliptic integral of the first kind. Evaluating Eq. (19) at $z=\pm 1$ gives a transcendental equation for the potential values at boundaries

$$\sqrt{\beta}=-\sqrt{\alpha_-}\{F_1[\psi(1)\sqrt{\alpha_+},\alpha_-]-F_1[\psi(-1)\sqrt{\alpha_+},\alpha_-]\}, \tag{20}$$

which complements Eqs. (14), (16), and (18) to produce a set of two transcendental equations for $\phi(\pm 1)$ that can only be solved numerically.

IV. NUMERICAL COMPUTATION AND RESULTS

Albeit $\alpha_{\pm}$ is complex, and thus elliptic integral of the first kind with complex variables is needed for this computation, the solutions are always real and are symmetric with respect to $\alpha_{\pm}$. We use a Newton-Picard method for the evaluation of the unknown surface field $\phi(1)$ and continuously vary the parameters β and μ with a continuation method. The pitchfork bifurcation of these antisymmetric solutions from the bifurcation point $\beta_c^{\mathrm{NS}}(\mu)$ of Eq. (12) is shown in Fig. 1 for different values of μ. It is evident that $\phi(1)$ first rises beyond a critical dimensionless separation β_c^{NS} and very rapidly reaches a constant asymptotic value $\phi^{\infty}(\mu)$ which depends only on μ at large separations, i.e., for large value of β. This asymptotic value is concomitantly reached when d' tends to -1, and $\alpha_{\pm}$ to 1 so that the arguments of the elliptic function in Eq. (19) reaches 1 where it display a unique logarithmic singularity to compensate for large value of β on the left-hand side. In this limit, one can evaluate the potential $\phi^{\infty}(\mu)$ from solving the simple transcendental equation,

$$[\mu(\phi^{\infty}-\phi_0)]^2=2(\cosh\,\phi^{\infty}-1), \tag{21}$$

found from Eq. (14). This value is illustrated for $\phi_0=0$ in Fig. 1. Furthermore, from knowing this value, it is easy to find the antisymmetric solution which is depicted for half of the domain in Fig. 2 for $\mu=2$.

One can see from this plot the unconfined charge distribution and long-range attraction of antisymmetric solutions.

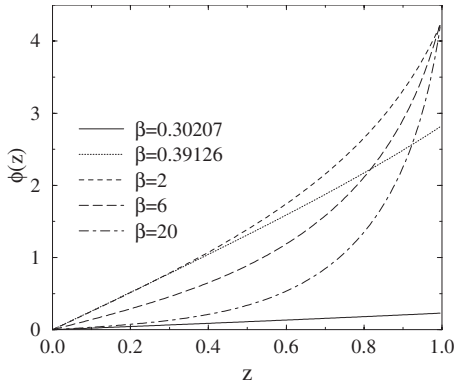

FIG. 2. Potential field versus distance z for different dimensionless gap values, $\mu=2$ and $\phi_0=0$.

For small values of β, the potential gradient at the origin $z=0$ monotonically increases with β. For a critical ratio of dimensionless half-gap β_m (e.g., equal to $\beta_m\simeq 0.391$ when $\mu=2$), this gradient at the origin reaches a maximum after which the potential profile starts to deform nonlinearly. Increasing β further more both decreases the potential gradient at the origin and increases it at the wall. When the surface potential at $z=1$ reaches the asymptotic value $\phi^{\infty}(\mu)$ solution of Eq. (21), the potential gradient at the wall monotonically increases with $\sqrt{\beta}$ according to Eq. (2).

A boundary layer develops near the wall with large potential gradient, while the potential rapidly decreases to zero away from the wall. The surface charge, which is proportional to the potential gradient, is then increasing as $\sqrt{\beta}$ leading to an asymptotic attractive force/potential at long range that will be subsequently studied in next section.

V. ATTRACTIVE BEHAVIOR

From knowing the surface potential one can easily deduce from Eq. (15) the negative pressure associated with isoelectric point antisymmetric solutions. This negative pressure is plotted in Fig. 3(a). The sharp maximum of the pressure in Fig. 3 is at the same value of β_m for which the potential gradient at the origin reaches a maximum [which is obvious from examining first relation (15)]. It is interesting to observe that the maximum force depends exponentially on the μ parameter. It might be a very sensitive way of estimating the parameter μ. When moving further apart from the isoelectric point, one finds that the attractive region exists only for a finite range of separation β which are larger than β_c^{NS}, as illustrated in Fig. 3(b). Repulsion due to native charges responsible for the effective Zeta potential ϕ_0 reduces the attractive region until it disappears completely beyond a critical ϕ_0. The repulsion also gives rise to a shallow maximum, a threshold pressure, as seen in Fig. 3(b). This leads to the "phase diagram" in Fig. 4(a) for the attraction/repulsion on the $\beta-\phi_0$ plane. Attractive interaction occurs near isoelectric points with minimum surface charge (low ϕ_0) and with high sensitivity of the condensation isotherm to external field (high μ). When attractive interaction is possible, a shallow threshold barrier exists except for nearly isoelectric conditions.

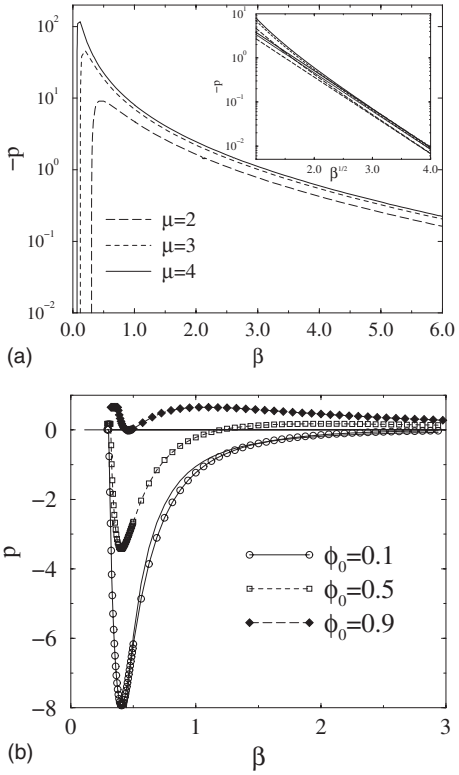

FIG. 3. (a) Semilogarithmic plot of the attractive force per unit surface p versus the square of the dimensionless half-gap β for different values of parameter μ and $\phi_0=0$. Inset: the corresponding large-gap asymptotic prediction (22) is shown with straight lines for each value of μ. (b) Same convention in usual coordinates for $\mu=2$ and three values of the compensate potential ϕ_0. The continuous curve shows a $-\beta^{-5/2}$ fit to one of the pressure variations.

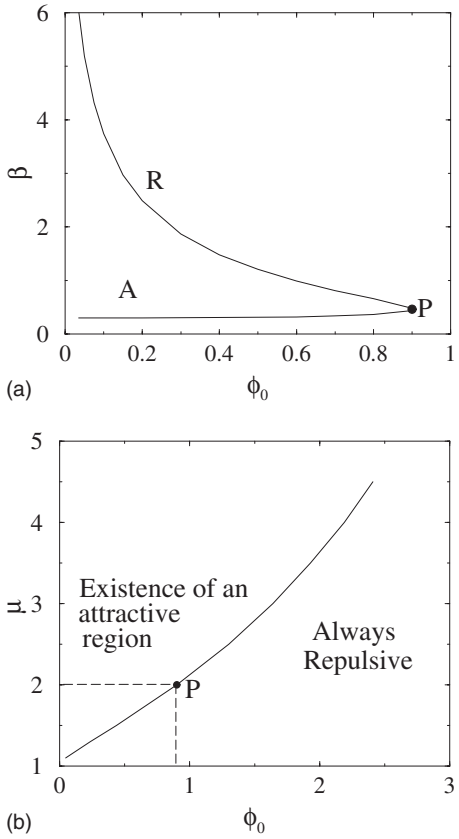

FIG. 4. Investigation of attractiveness in the phase space of the parameters of the problem. (a) $(\beta-\phi_0)$ plane for $\mu=2$. R stands for repulsion and A for attraction. Point P ($\beta\simeq0.465$, $\phi_0\simeq0.9$) corresponds to the minimum equal to zero of the pressure curve represented in Fig. 3(b) (b) $(\mu-\phi_0)$ plane. Long-dashed lines locate point P in this plane.

As previously discussed, the large-gap limit is interesting to consider and compare to the usual (D-H) limit for the force. In this limit, the parameter d' approaches value of -1, which corresponds to the vicinity of the logarithmic singularity of the elliptic function. Using known asymptotic behavior of the elliptic function near this singularity, it is possible to evaluate analytically the force distribution using Eqs. (14), (15), and (19),

$$\text{for } \beta \gg 1 \quad p \sim -\exp(-2\sqrt{\beta}) \sim -\exp(-2h/\lambda). \qquad (22)$$

We compare this asymptotic behavior against the numerical results in the inset of Fig. 3(a) and show very good agreement for β values as small as 3. This asymptotic force is also consistent with our numerical values for both attractive or repulsive long-range forces when $\phi_0\neq0$ (not shown). It is interesting to note that the slope of the curves is independent of μ, as predicted by Eq. (22) and is consistent with the constant asymptote of the surface potential at large separation in Fig. 1.

VI. COMPARISON WITH EXPERIMENTS

A. Derivation of Stern-layer parameters from adsorption isotherm linearization

In this section we use the "classical" derivation for Stern-layer parameters from adsorption isotherm linearization. We evaluate the μ and ϕ_0 parameters from the isotherm proposed in Zohar *et al.* [1] for the net surface charge density σ at different trivalent Cobalt-hexamine concentrations. The isotherm is derived from simple mass-action kinetics whose parameters are either measured or estimated with simple arguments, shown to be inconsistent with phase-locked Wigner crystals

$$\sigma(\phi) = -n_{Si}e\frac{1-K_1[Co]\exp(-3\phi)}{1+K_2[Co]\exp(-3\phi)}, \qquad (23)$$

where e is the electron charge, [Co] the Cobalt-hexamine concentration, ϕ the dimensionless potential rescaled by RT/ZF, $K_1=10^4$ and $K_2=5\times10^3$ M^{-1} are two empirical constants related to the association and dissociation rates, and n_{Si} is the density of ionizable silanol groups which is estimated to range between $n_{Si}\simeq0.3-1$ nm^{-2}. The surface electroneutral condition $\sigma(\phi_0)=0$ leads to a simple dependence between the compensated Zeta potential ϕ_0 at a particular counterion concentration,

$$\phi_0 = \frac{\ln(K_1[Co])}{3}. \qquad (24)$$

A first-order Taylor expansion of Eq. (23) about this reference point leads to

$$\sigma(\phi) \simeq -2n_{\mathrm{Si}}e(\phi-\phi_0). \tag{25}$$

The application of Gauss theorem at the surface location $z=1$, for dimensionless potential rescaled by $RT/ZF=k_BT/Ze$ leads to

$$\partial_z\phi = -2\frac{Ze}{k_BT}\frac{n_{\mathrm{Si}}eh}{\epsilon}(\phi-\phi_0). \tag{26}$$

From identifying the constant of this affine relation to Stern condition (2) with $K=-\mu h/\lambda$ one finds

$$\mu = 2Z\ell_B\lambda n_{\mathrm{Si}} \tag{27}$$

where, again, $\ell_B \equiv e^2/\epsilon k_BT$ is the Bjerrum length. It is then interesting to compare Eq. (27) with the previous expression derived from the theoretical two-fluid model of Lau *et al.* in Eq. (7). The condensed ion density n_C in the theoretical derivation of constant μ proposed in Eq. (7) is replaced by the density of ionizable silanol groups n_{Si} in its empirical counterpart given in Eq. (27). Since they both represent the surface density of negative charges at the solid surface, this gives a consistent picture of how the parameter μ is related to physical constants. Moreover, since n_C is a theoretical prediction of the surface charge density (which could be related to other physical parameters from charge condensation mechanism as explained in [22]) where n_{Si} is related to an experimental estimate of the same quantity, both expressions are fully consistent with either a theoretically or an experimentally derived expression for μ. Finally, it is hence surprising that such different approaches for estimating parameter μ only quantitatively differ by a prefactor which is $2Z$ in one case and πZ^2 in the other case. The different dependence with the valency Z could be attributed to the fact that in the experimental case, the negative charges associated with silanol groups are generally considered as monovalent.

The range of possible experimental value for n_{Si} leads to $\mu=1.32-4.4$. Furthermore relation (24) produces negative values of ϕ_0 for these experimental conditions. However, as the problem is invariant with the transformation $(z,\phi,\phi_0) \rightarrow (-z,-\phi,-\phi_0)$, our results obtained for positive ϕ_0 also apply for negative ones.

B. Comparison with experimental force

The configuration which is analyzed in this paper is associated with two parallel identical surfaces. Nevertheless, the available experimental fine measurements of the force between similar surfaces in an electrolyte have all been performed with AFM [1,2,4]. Those measures are associated with sphere/plane configurations. Nevertheless some features of the predicted attraction force between two parallel planes can be possibly extended when the ratio between the AFM tip distance to the wall to its radius of curvature is small [4,20,23]. A first possible direct comparison between theory and experiments can be found from analyzing the far-field behavior of the force which in both cases should be the same up to some irrelevant prefactors [23].

1. Long-range behavior

As mentioned earlier in Sec. I, different theoretical predictions have been proposed for the long-range behavior of the possibly attractive force of an electrolyte confined between two identical walls distant by a half-gap h. Nevertheless, few of these predictions have been successfully compared with experiments but the modified exponential attraction,

$$p \sim \frac{\exp(-4h/\lambda)}{2h}, \tag{28}$$

has been proposed in [19,20] and experimentally tested in [4].

Nevertheless, there might be some caution for a definite answer to this question since the proposed modified exponential behavior very slightly differs from a pure exponential behavior more recently reported in [1,2]. Nevertheless, to our knowledge, the possibility of non-exponential, algebraic far-field decay proposed in [8,10,18] has never received any convincing experimental evidence. Furthermore, since most of the experimental evidence for a modified exponential attraction are tested on semilogarithmic coordinates in [4], and given the fact that experimental observation are also relatively noisy, it is hard to draw a definite conclusion on a possible logarithmic corrections to a mere linear trend of $\ln p$ versus h in Eq. (28). Moreover, most of the correction to the linear behavior in Fig. 2 of [4] are concentrated in the close region where it is highly possible that the far-field asymptotic regime broke down.

On the contrary, our exponential decay of long-range attraction (22) is consistent with various experimental observations [1,2]. To the best of our knowledge, our approach is the only one which predicts a pure exponential asymptote for the attractive force found in [2]. We verify this statement by analyzing the slope of the exponential decay of the experimental measurements of [2]. To compare more quantitatively the current theory between two planar surfaces to that between an AFM tip (an attached spherical bead) and a flat surface in the experiment, an averaging over the AFM tip is carried out. The justification of this approximation in the framework of a rigorous asymptotic lubrication approach can be found in [23]. Furthermore, the computation of the macroscopic force which is experienced by the AFM tip necessitates the knowledge of the local pressure dependence $p[h(r)]$ versus the local distance $h(r)$ between the plane surface and the AFM tip. In principle, with this dependence being nonanalytic, its computation necessitates some numerical integration as performed in [23]. A shortcut to this more complete computation is to find some simple expression for the pressure dependence with $h(r)$ which reasonably fits the far-field behavior of the pressure dependence with h displayed in Figs. 3.

A very good estimate of the pressure dependence with dimensionless half-gap β is $p(\beta) \simeq \beta^{-5/2} = (h/\lambda)^{-5}$ as illustrated in Fig. 3(b). Averaging this pressure from the true tip separation h_m to infinity where the interaction vanishes and setting it equal to the pressure of an equivalent separation between two planes,

$$P(\langle h\rangle/\lambda) = \left(\frac{\langle h\rangle}{\lambda}\right)^{-5} = \int_{h_m/\lambda}^{\infty} h^{-5}dh = \frac{1}{4}\left(\frac{h_m}{\lambda}\right)^{-4}, \tag{29}$$

one gets a dimensionless equivalent half-gap separation of

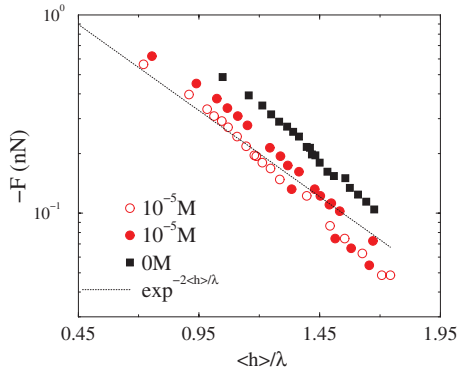

FIG. 5. (Color online) Test of the long-range scaling (22) for the data collected from Fig. 1(b) of [2] associated with different concentrations of $LaCl_3$ salt with an adjusted equivalent half-mean separation $\langle h\rangle$. The experimental Debye-length values λ are those given in [2].

$$\frac{\langle h\rangle}{\lambda} = 4^{1/5}\left[\frac{h_m}{\lambda}\right]^{4/5}, \tag{30}$$

whose variation with the initial minimum distance h_m is almost linear. Using the equivalent gap $\langle h\rangle$ deduced from the observed h_m from Eq. (30), associated with $LaCl_3$ salt analyzed in [2], we plot in Fig. 5 the experimental pressure as well as our theoretical prediction $p \sim \exp[-2\langle h\rangle/\lambda]$. The resulting slope in log-linear scale very satisfactorily compared with our theoretical prediction as previously stated in relation (1) in the paper of Besteman *et al.* [2] independently of parameter μ. Hence not only our prediction quantitatively agrees with a pure exponential decay but the observed slope in semilogarithmic representation also leads to satisfactory comparison with experimental data.

2. Intermediate distance force

We can carry on this approximation within intermediate separation distances as well as when varying the concentration conditions. To make a possible link between some experimental conditions and theoretical predictions, one needs to evaluate the Stern-layer parameters μ and ϕ_0. This is not possible with the data of Besteman *et al.* [2] since no absorption isotherm is given for their experimental conditions, but this is possible with the data of Zohar *et al.* [1] as was done in Sec. VI A.

We choose the cross-section area of the spherical AFM tip at a separation of two Debye lengths as a reference area to calculate the force such that

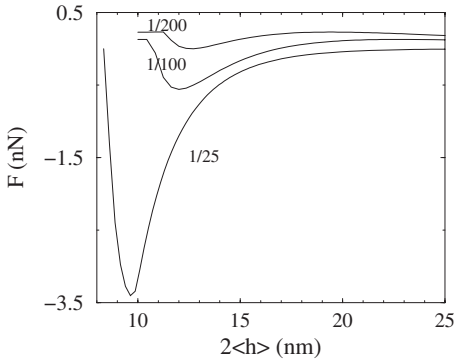

FIG. 6. Plot of the predicted dimensional force F (31) for λ =10 nm; three values of Cobalt-hexamine concentration relative to NaCl 1/200, 1/100, and 1/25 which corresponds to 4.5×10^{-6}, 9×10^{-6}, and 9.6×10^{-5} M and gives the following compensated Zeta potential $\phi_0=-1,-0.8,-0.013$ analyzed in Fig. 2 of [1], using a density of ionizable silanol groups $n_{Si}=0.48$ nm^{-2} leading to $\mu=2.14$. No adjustable parameter has been used.

$$F = 4\pi R\lambda\epsilon\left(\frac{k_BT}{Ze\lambda}\right)^2 p, \tag{31}$$

with the AFM tip radius $R=510^{-6}$ m, the liquid permittivity $\epsilon=80\epsilon_0$, and the temperature at 293 K represented in Fig. 6. They display the same qualitative trends and variations as the measured ones in Fig. 2 of [1] and are quantitatively consistent within the same order of magnitude. Hence, our predictions not only lead to an accurate estimate of the asymptotic long-range decay of the force but they also give consistent intermediate distance behaviors.

VII. CONCLUSION

We have shown that it is possible to obtain an attractive antisymmetric solution for the potential distribution of an electrolyte between two identical surfaces by taking into account the coupling between surface charge across the double layer due to the effect of each field on the condensation of polyvalent counterions on the other, as captured by a simple linear Stern condition derived from common isotherms obeying mass-action kinetics. We show analytically that asymmetric charge inversion and attraction are possible, and we produce numerical results that are qualitatively and quantitatively consistent with experimental data. Our results reconcile correlated fluctuation theory based attraction, Stern-layer models, and available experimental observations.

ACKNOWLEDGMENTS

We are grateful for inputs from Y. E. Zhu, X. Cheng, C. Beaume, and S. Basuray, and fruitful discussions with Pr. E. Trizac.

[1] O. Zohar, I. Leizerson, and U. Sivan, Phys. Rev. Lett. **96**, 177802 (2006).
[2] K. Besteman, M. A. G. Zevenbergen, H. A. Heering, and S. G. Lemay, Phys. Rev. Lett. **93**, 170802 (2004).
[3] P. M. Claesson and H. K. Christenson, J. Phys. Chem. **92**, 1650 (1988).
[4] P. Kékicheff and O. Spalla, Phys. Rev. Lett. **75**, 1851 (1995).
[5] W. M. Gelbart, R. Bruinsma, P. Pincus, and V. Parsegian, Phys.

Today **53** (9), 38 (2000).
[6] J. C. Neu, Phys. Rev. Lett. **82**, 1072 (1999).
[7] X. Cheng and H.-C. Chang (private communication).
[8] D. B. Lukatsky and S. A. Safran, Phys. Rev. E **60**, 5848 (1999).
[9] R. R. Netz and H. Orland, Eur. Phys. J. E **1**, 203 (2000).
[10] A. W. C. Lau and P. Pincus, Phys. Rev. E **66**, 041501 (2002).
[11] A. W. C. Lau, Phys. Rev. E **77**, 011502 (2008).
[12] F. Oosawa, Biopolymers **6**, 1633 (1968).
[13] N. Gronbech-Jensen, R. J. Mashl, R. F. Bruinsma, and W. M. Gelbart, Phys. Rev. Lett. **78**, 2477 (1997).
[14] J. G. Kirkwood and J. B. Shumaker, Proc. Natl. Acad. Sci. U.S.A. **38**, 855 (1952).
[15] R. James and T. W. Healy, J. Colloid Interface Sci. **40**, 42 (1972).
[16] L. Dai, Y. Mu, L. Nordenskiold, and J. R. C. van der Maarel, Phys. Rev. Lett. **100**, 118301 (2008).
[17] A. Y. Grosberg, T. T. Nguyen, and B. I. Shklovskii, Rev. Mod. Phys. **74**, 329 (2002).
[18] P. Attard, R. Kjellander, and D. J. Mitchell, J. Chem. Phys. **89**, 1664 (1988).
[19] R. Podgornik, J. Chem. Phys. **91**, 5840 (1989).
[20] O. Spalla and L. Belloni, Phys. Rev. Lett. **74**, 2515 (1995).
[21] L. Belloni and O. Spalla, J. Chem. Phys. **107**, 465 (1997).
[22] A. W. C. Lau, D. B. Lukatsky, P. Pincus, and S. A. Safran, Phys. Rev. E **65**, 051502 (2002).
[23] F. Plouraboué and H.-C. Chang (unpublished).